Lamellar Thickness Distributions in Linear Polyethylene and Ethylene Copolymers

L. Lu, R. G. Alamo, and L. Mandelkern*

Department of Chemistry and Institute of Molecular Biophysics, Florida State University, Tallahassee, Florida 32306-3015

Received April 11, 1994; Revised Manuscript Received July 26, 1994®

ABSTRACT: Crystallite thickness distributions have been calculated using the Thomson–Gibbs equation from the endotherms obtained by differential scanning calorimetry. These distributions were then compared with those obtained by transmission electron microscopy or by Raman spectroscopy (LAM). For linear polyethylene, the experimentally measured distribution can only be reproduced by choosing appropriate combinations of the interfacial free energy and the heating rate. The distributions calculated from endotherms of random ethylene copolymers are very different from those that are obtained directly. The nature of the fusion process of random copolymers, where the free energy of the melt is not invariant with temperature, restrains the applicability of the simple Thomson–Gibbs equation.

Introduction

The lamellar thickness distribution in crystalline polymers in general, and in the polyethylenes in particular, is an important factor to consider when interpreting macroscopic properties. Differences in lamellar size distributions may account for considerable differences in thermal and mechanical properties that can be found in polyethylenes having identical levels of crystallinity and molecular weight. There are several different experimental methods that can be used to determine the thickness distributions. These include transmission electron microscopy,[1–3] analysis of the longitudinal acoustic mode (LAM) in Raman spectroscopy[1,3–6] and small angle X-ray scattering.[2,7] Lamellar, or crystallite, thickness distributions have also been calculated from the endotherms obtained by differential scanning calorimetry (DSC) using the well-known Thomson–Gibbs equation.[8–13]

The DSC endotherms give a distribution of melting temperatures that in principle can be converted to a distribution of crystallite thicknesses by means of the relation

$$T_m = T_m^\circ \left(1 - \frac{2\sigma_e}{\Delta H_u L}\right) \qquad (1)$$

Equation 1 is the variant of the Thomson–Gibbs equation for a lamellar crystallite of large lateral dimensions and finite thickness. It is a very general expression that is independent both of the nature of the molecules involved in forming the crystallite and of the interfacial structure. Thus, it is valid for either monomeric or polymeric species. This relation is not unique to polymer crystallites with supposed regular chain folding.[14,15] In this equation T_m is the observed melting temperature of a lamellar crystallite of thickness L, T_m° is the equilibrium melting temperature of the infinitely thick crystal, σ_e is the interfacial free energy associated with the basal plane, and ΔH_u is the enthalpy of fusion per repeating unit. In the analysis it is further assumed that the rate of heat flow, at a given temperature, is proportional to the fraction of lamellae that has a thickness L.

Different investigators have applied eq 1 directly to DSC endotherms and calculated the lamellae thickness[16–19] and the thickness distributions of linear polyethylene[9,10] and ethylene copolymers.[11–13,16] However, in none of these studies were the thickness distributions calculated from the DSC experiment compared with those obtained by a direct experimental measurement of the distribution. In some of these works, long periods from SAXS patterns were obtained and matched with the calculated most probable value in the distribution.[9,13]

In the present work the lamellar thickness distributions of linear polyethylenes and random ethylene copolymers have been calculated from DSC data according to eq 1. These results were then compared with the distributions obtained directly from either Raman spectroscopy or transmission electron microscopy utilizing the same sample. This is the first time that a direct comparison of the complete distribution has been made between the calorimetric method and any other.

Experimental Section

Materials and Crystallization Conditions. The molecular characteristics of the linear polyethylene and ethylene copolymers used in this work are summarized in Table 1. The linear polyethylene fraction designated A was obtained from the Society des Petroles D'Aquitaine. The one designated B is a reference standard obtained from the National Bureau of Standards. They both have very narrow molecular weight distributions, as indicated by their weight to number average molecular weight. Sample C is a very high molecular weight whole polymer obtained from the Hercules Powder Co.

Four different random ethylene copolymers (D–G) were also used. Hydrogenated poly(butadiene), sample F, was obtained from the Phillips Petroleum Co. It has a very narrow molecular weight distribution, homogeneous composition, and a random distribution of the ethyl branches. The ethylene–butene (EB) (sample D) and ethylene–hexenes (EH) (samples E and G) are typical of those previously studied in this laboratory.[20,21] They have narrow compositions and most probable molecular weight distributions. Copolymers with different comonomer contents were chosen to ascertain the effect of increasing branching content on the thickness distributions calculated from the DSC thermograms.

All but one of the samples were crystallized from the melt under crystallization conditions ranging from very rapid crystallization into a mixture of either liquid N_2 and *n*-pentane (−130 °C) or one of dry ice and isopropyl alcohol (−78 °C) to isothermal crystallization or slowly cooling from the melt (150–180 °C) to room temperature. The slow cooling process usually took between 4 and 6 h. Crystals from sample B were formed from a relatively concentrated solution in decalin at a crystallization temperature of 102 °C. Other details of the crystallization conditions are included in Table 1.

* Abstract published in *Advance ACS Abstracts*, September 15, 1994.

0024-9297/94/2227-6571$04.50/0

Table 1. Molecular Characteristics and Crystallization Conditions of the Samples Studied

designation	mol % branch points	$10^{-3}M_w$	M_w/M_n	crystallization conditions
		Linear Polyethylenes		
A	0	80.8	1.05	T_c = 118 °C
B	0	119	1.19	v_2 = 0.35 (decalin) T_c = 102 °C
C	0	8000[a]		quenched, −130 °C
		Ethylene Copolymers		
D	1.18	106	≈2	slowly cooled
E	1.21	104.5	2.4	quenched, −78 °C
F	2.20	108	1.3	quenched, −78 °C
G	2.64	88	2.0	slowly cooled

[a] Viscosity average molecular weight.

Techniques. A Perkin–Elmer DSC-2B differential scanning calorimeter was used to record the melting process. Films of similar shape and thickness were used to avoid possible differences in the shape of the DSC melting peak with sample geometry. The samples were scanned at the heating rates of 5, 10, 20, and 40 °C/min. Temperature calibration was carried out with indium. The melting curves were digitized with a temperature interval of 0.1 deg or narrower and converted into ordered sequence length distributions using eq 1. To compute the distribution of lamellae thicknesses, a tilt angle of 30° was taken between the sequence length and the surface of the lamellae. For the linear polyethylene chain the value of $T_m°$ was taken as 145.5 °C and 2.8×10^9 erg/cm^3 was taken for the enthalpy of fusion (ΔH_u).[22,23]

Raman spectra in the range 5–60 cm^{-1} were recorded on a SPEX 1403 double monochromator spectrometer. The samples were illuminated by an argon ion laser beam at 514.5 nm. The power at the sample was 80–100 mW with the scattered light being collected at a 90° angle to the exciting beam. The LAM bands were analyzed according to the method proposed by Snyder and Scherer[4] to yield the ordered chain sequence length, L_R, and its distribution. A value of 2.9×10^{11} dyn/cm^2 was used for the elastic modulus of the ordered polyethylene chain.[24] The lamellar core thickness, L_C, was calculated from the ordered chain sequence length by correcting for a chain tilt of 30°.[25] The electron microscopic techniques and accompanying analysis have been described in detail in previous publications.[2,3,26,27]

Results and Discussion

Linear Polyethylene. The lamellar thickness distributions of samples A and B were studied by both thin section electron microscopy and Raman (LAM). These results were also reported in a previous communication where a detailed comparison was made between the two experimental methods for sample A.[1] It was concluded that a good quantitative agreement is obtained between both methods when account is taken of the chain tilt and the distribution is narrow.

To compare these distributions with the one calculated from DSC melting endotherms, an identical sample (sample A) was melted at a heating rate of 10 °C/min. From the DSC traces, the thicknesses along the melting curve were calculated using eq 1. Figure 1 compares the normalized distributions obtained from electron microscopy and Raman LAM[1] with the one obtained from DSC for fraction A crystallized at 118 °C for 2 min. In this calculation the reasonable values of σ_e of 2000 and 2500 cal/mol were taken.[28] The distributions obtained from the Raman LAM and from electron microscopy are essentially identical to one another. The thickness distribution calculated from the DSC shifts to higher values and becomes slightly broader with increasing values of σ_e. The calculated distribution gives a good agreement with the independently obtained actual distribution when an appropriate value is selected for σ_e. At the heating rate

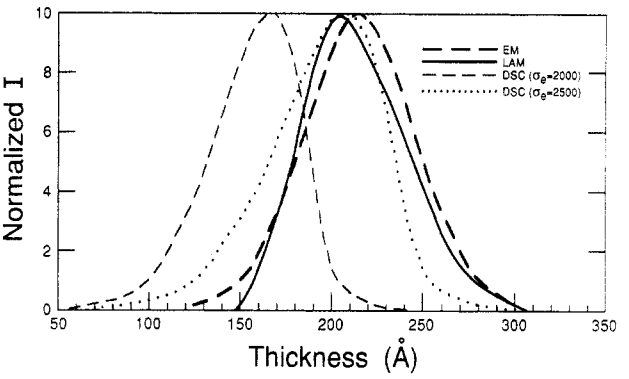

Figure 1. Normalized crystallite thickness distributions of sample A crystallized at 118 °C for 2 min. The thin dashed and dotted curves correspond to the calculated distributions according to eq 1 for the indicated values of σ_e. The EM and LAM distributions were taken from ref 1.

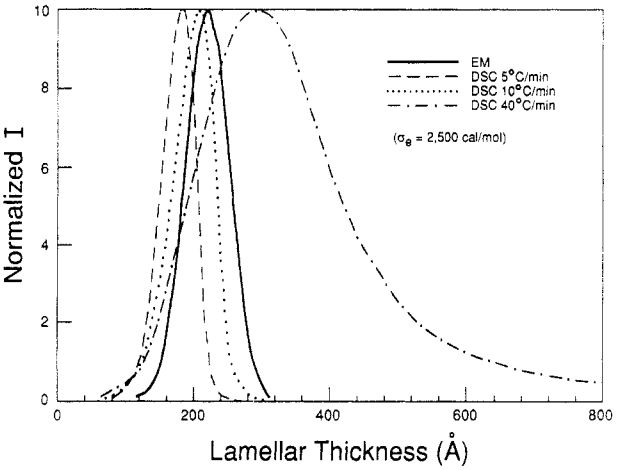

Figure 2. Calculated lamellae thickness distributions according to eq 1 from the DSC melting peaks of sample A crystallized at 118 °C for 20 min and obtained at the indicated heating rates. The thickness distribution obtained from thin section electron microscopy is also indicated.

used, 10 °C/min, this value is estimated to be 2580 cal/mol for the sample studied.

In order to investigate the influence of heating rate on the distribution that is deduced from a thermogram, the thickness distribution, for a given value of σ_e, was also obtained at an arbitrary heating rate. Calculated distributions using different heating rates are plotted in Figure 2 for sample A crystallized at 118 °C for 20 min. A fixed value of σ_e = 2500 cal/mol was used in these examples. A constant temperature calibration, similar to calibrations used previously,[9] was used for each heating rate on the basis of the onset melting temperature of indium. The endotherms obtained with heating rates of either 5 or 10 °C/min lead to distributions that are close to those from either electron microscopy or the LAM. However, increasing heating rates broadens the calculated distribution and moves it toward very high thicknesses.

Figure 3 illustrates a similar analysis for dried crystallites of sample B that were obtained from a concentrated solution. The choice of σ_e = 2300 cal/mol allows for an excellent match, at a heating rate of 10 °C/min, between the calculated distribution and that obtained from the LAM. A lower value of σ_e (2150 cal/mol) will permit a close fit for the curve obtained at a heating rate of 20 °C/min, and a higher value of σ_e (2500 cal/mol) will do the same for that obtained at 5 °C/min. However, no choice of a σ_e value can be made that will fit the distribution obtained with the 40 °C/min heating rate.

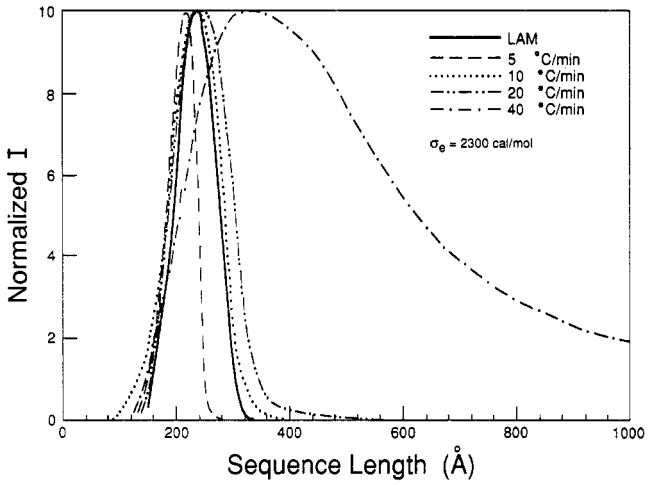

Figure 3. Calculated sequence length distributions according to eq 1 from the DSC melting peaks of dried crystals of sample B. The crystals were run at the heating rates indicated in the figure. The distribution obtained from the LAM and the σ_e value used in eq 1 are also indicated.

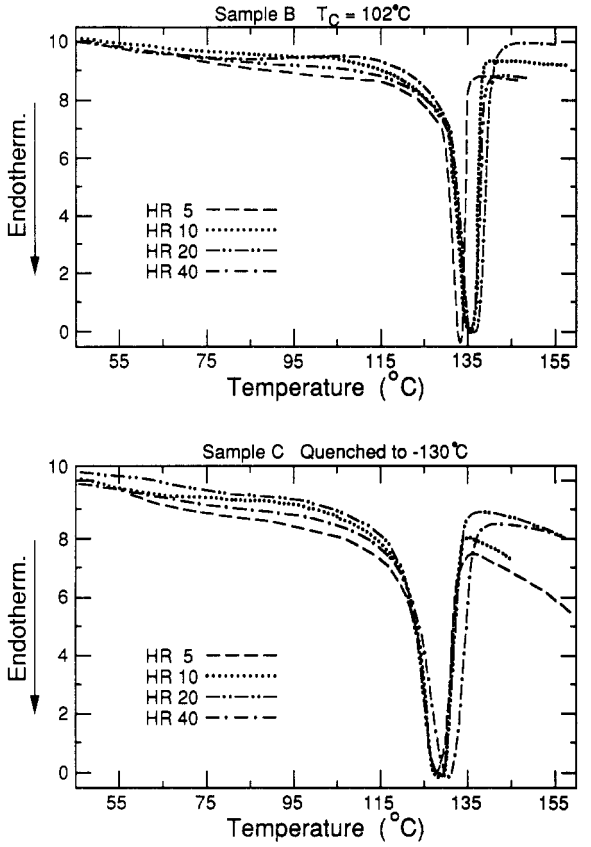

Figure 4. Normalized DSC melting curves of samples B and C obtained at the heating rates indicated in the thermograms.

No effects of heating rate were observed with the very high molecular weight linear polyethylene (sample C) for heating rates between 5 and 40 °C/min. The thickness distribution calculated from the thermogram could be matched quite well to that obtained from the LAM for σ_e values between 2000 and 3000 cal/mol.

It might appear that the larger thicknesses calculated at the high heating rate in Figure 2 and 3 are due to superheating effects and that sample C, crystallized rapidly, does not show any superheating. However, this possibility is ruled out by looking at the actual endotherms (Figure 4) obtained at different heating rates for samples B and C. The peak temperature and the width of the endotherm shift to higher temperatures with increasing

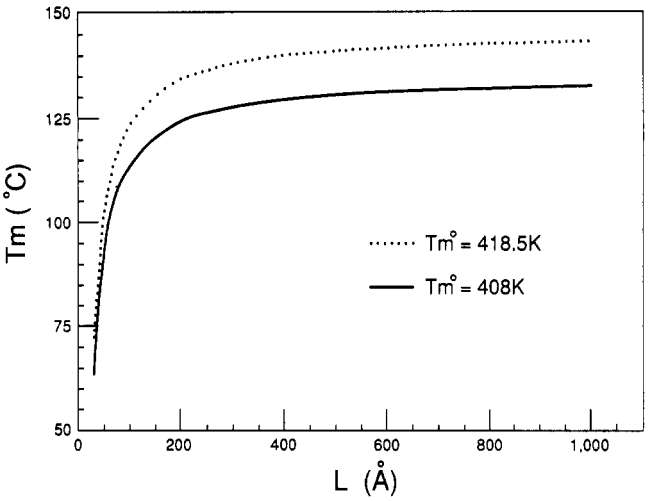

Figure 5. Calculated T_m according to eq 1 for two different values of the equilibrium melting temperature ($T_m°$). A constant σ_e = 2000 cal/mol was used in the calculations.

heating rate, but a comparison between heating rates of 10 and 40 °C/min indicates that the shift is of about the same magnitude (2–3 deg) for both samples. A similar degree of superheating is, therefore, expected on the basis of these thermograms. The reason for the differences in the calculated distributions using eq 1 for a heating rate of 40 °C/min, between sample B (with unreasonable high thickness values) and sample C (which shows reasonable values matching the LAM distribution) can be attributed to the actual melting temperatures observed in the fusion experiment. In the examples shown in Figure 4, sample B (upper thermogram) shows a melting temperature range (at 40 °C/min) between 115 and 143 °C and that for sample C (lower thermogram), at the same heating rate, is between 110 and 138 °C. As a consequence of the high sensitivity of eq 1 at melting temperatures approaching $T_m°$, the calculated distribution from endotherms covering a range of temperatures close to $T_m°$ will be much broader and toward much higher thicknesses than the distribution from a similar endotherm covering a lower melting temperature range.

To illustrate this latter point, T_m values were calculated according to eq 1 for arbitrary values of L. The calculations were carried out for a σ_e of 2000 cal/mol and two different values of $T_m°$, one corresponding to linear polyethylene and a second $T_m°$ about 10 deg lower. The calculated T_m values are plotted against L in Figure 5. It is clear that the range of temperatures where sample C melts (all heating rates included) covers a relatively narrow range of calculated L values, between 80 and 350 Å in the upper curve of Figure 5. This also holds for the endotherms of sample B obtained at 5, 10, and 20 °C/min. However, the endotherm of sample B obtained at 40 °C/min extends up to temperatures of 143 °C. As is shown in Figure 5, the region of temperatures between 140 and 143 °C covers a very wide range of calculated thicknesses (from about 400 to over 1000 Å). In this temperature range, small variations in T_m lead to very large variations in the calculated thickness.

From these results we can conclude that the use of the Thomson–Gibbs equation to calculate the thickness distributions of linear polyethylenes from DSC thermograms is feasible if the value of σ_e is known and the heating rate is restricted to about 10 °C/min.

The question could be raised as to whether the shape of the true endotherm is altered by a melting–recrystallization process. However, this possibility can be ruled

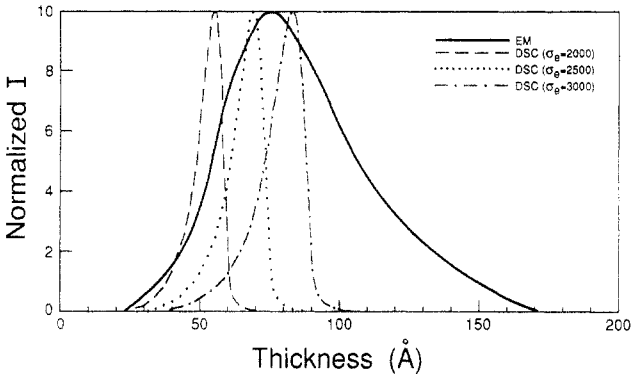

Figure 6. Normalized crystallite thickness distributions for sample D. Dashed and dotted curves are calculated distributions from the DSC melting peak, according to eq 1, for the indicated values of σ_e. The distribution obtained from electron microscopy (EM) is also shown.

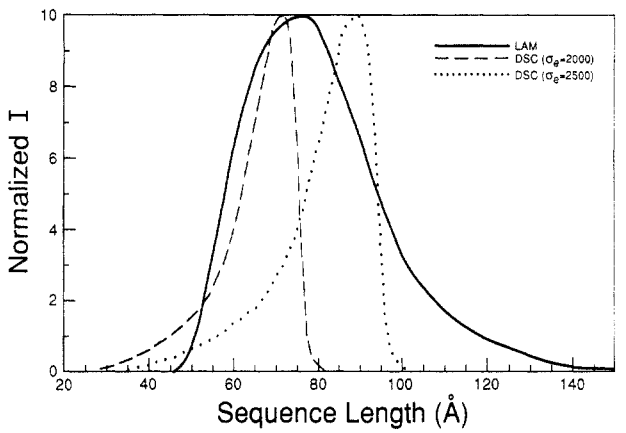

Figure 7. Same as Figure 6 for sample E. The distribution obtained from the LAM of the Raman spectrum is shown in this figure.

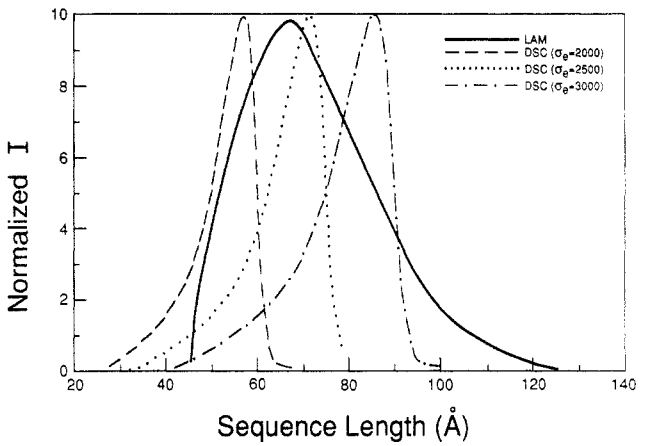

Figure 8. Same as Figure 7 for sample F (a hydrogenated polybutadiene with 2.2 ethyl branches per 100 total carbons).

out. The samples studied in Figures 1–3 have distributions ranging from about 140 to 310 Å and centered around 215–220 Å. Previous studies have shown that such relatively thick crystals do not undergo melting with further recrystallization during the fusion process.[29,30]

The calculations shown in Figures 1–3 point out that if the thickness distribution of a linear polyethylene is known, it can be fitted with that calculated from a DSC thermogram, by the appropriate choice of σ_e, provided superheating effects are not a major consideration. However, if the distribution is not known, the one that is calculated from the thermogram is subject to the choice of σ_e and heating rate.

Ethylene Copolymers. We will first analyze the results for the two ethylene copolymers that contain the smallest amounts of comonomer. The ethylene–butene sample with 1.18 ethyl branches per 100 carbons (sample D) was slow cooled from the melt, while the ethylene–hexene copolymer, which has about the same molecular weight (100 000) and a similar co-unit content (sample E), was rapidly quenched to −78 °C. For both of these copolymers, the ethyl and butyl branches are excluded from the crystal lattice.[20,21,31,32] When compared to linear polymers, random copolymers melt over a much broader temperature range because of the wide distribution of sequence lengths in the residual melt, which change, as fusion progresses.[31–34] Thus, the equilibrium melting temperature will be very difficult, if not impossible, to determine from experiments.[33,34] In addition, it has been shown that the T_m/T_c extrapolation method, which is commonly used to obtain the equilibrium melting temperatures of polymers, cannot be applied to random copolymers.[35] The equilibrium melting temperature was then calculated from the Flory theory,[31,34] which is appropriate when the crytalline phase remains pure.

The thickness distributions of these two copolymers were calculated from their respective thermograms, taking for σ_e values ranging from 2000 to 3000 cal/mol. The results are compared with the distributions obtained from electron microscopy in Figure 6 for sample D and from the Raman LAM in Figure 7 for sample E. For either case the distributions calculated from the melting curves do not reproduce the actual thickness distributions for the heating rate of 10 °C/min that was used in these examples. The width at half-height is 2–4 times narrower than the actual distributions determined from either electron microscopy or the Raman LAM. Increasing the value of σ_e causes the distributions to become broader and to shift to higher values of the thicknesses. In order to reproduce the breadth of the distribution that is found experimentally, excessively high values of σ_e are needed. If this procedure is followed, distributions that are centered at unrealistic large thicknesses are obtained.

It is also of interest to compare the thickness distributions obtained from DSC and Raman or TEM of copolymers of higher co-unit content such as samples F and G. It is known that the fusion range becomes broader with increasing co-unit content in the copolymer.[36] In Figure 8 the calculated distribution of sample F, a hydrogenated poly(butadiene) (equivalent to ethylene–butene) with 2.2 mol % branch points is compared with the one obtained from the Raman LAM. The distributions from the endotherm were calculated for σ_e values ranging from 2000 to 3000 cal/mol. We find that the calculated distributions are much narrower than the one directly observed from the LAM. Although the melting range is broad the calculated distribution is unrealistically narrow. A σ_e of 2500 cal/mol gives a peak value that corresponds to the most probable value in the Raman distribution; however, the shape of the distribution is not reproduced. Unreasonably low values of σ_e (800 cal/mol) and $T_m°$ (112 °C) would be needed in order to obtain a close match to the LAM distribution.

A similar example is given in Figure 9 for an ethylene–hexene copolymer with 2.64 mol % butyl branches (sample G) that was slowly cooled from the melt. The distributions calculated from the melting endotherm, which was obtained at 10 °C/min, are well removed from representing the one obtained by electron microscopy. Although the most probable thickness values can be matched, the complete distribution cannot.

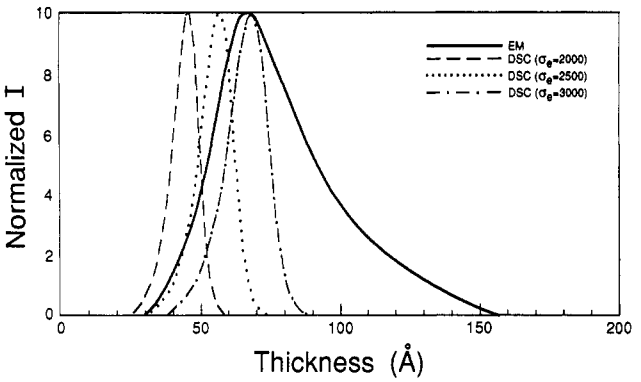

Figure 9. Same as Figure 6 for sample G (an ethylene–hexene copolymer with 2.64 butyl branches per 100 total carbons).

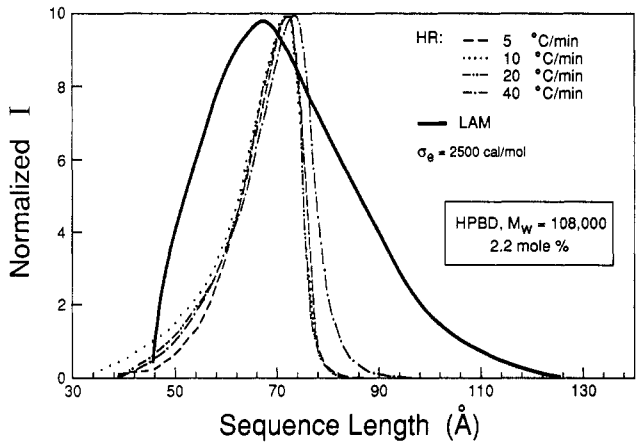

Figure 10. Comparison of the ordered sequence length distribution obtained from the LAM and those calculated from DSC melting curves obtained at different heating rates for sample F. The heating rates and the σ_e value used in the calculations are indicated.

The copolymer thermograms that have been analyzed up to now were all obtained at a heating rate of 10 °C/min. Since it was found previously that for the linear polyethylenes the heating rate had a profound effect on the calculated distribution, a similar situation is initially expected for the copolymers. Thus, the influence of heating rates on the distributions that are calculated for random copolymers is illustrated in Figure 10 for the hydrogenated poly(butadiene) (sample F). The melting thermograms were recorded at rates ranging from 5 to 40 °C/min, and the distributions were calculated taking σ_e = 2500 cal/mol and $T_m°$ = 137.5 °C.[34] There is essentially no difference in the distributions calculated from the thermograms obtained at 5, 10, or 20 °C/min. The peak values and breadths are essentially identical. The distribution calculated from the 40 °C/min thermogram differs only minutely from the others. It is slightly broader and shifted to somewhat higher thicknesses. However, the small differences found in the analysis of the copolymers are trivial when compared with the major changes found with the linear polyethylenes.

Darras and Seguela[13] have also calculated the crystalline lamellae thickness distribution of a set of ethylene–butenes from DSC traces. The value of σ_e used was obtained by identifying the most probable value of the distribution to the crystallite thicknesses deduced from the small angle X-ray scattering long period. Since no additional effort was made to obtain the distribution by direct methods, we can conclude, on the basis of our results, that the calculated distributions were much narrower than the actual ones.[37]

Several major problems are thus encountered in the determination of the crystallite thickness distribution of copolymers from DSC endotherms. One is that a reasonable representation of the actual crystallite distribution cannot be obtained at any heating rate or by changing the σ_e value. Another is that essentially the same distribution is obtained irrespective of the heating rate used. The lack of an adequate representation of the distribution can be attributed to the use of eq 1. The underlying premise in applying the Gibbs–Thomson equation is that, besides the usual specific heat effect, the free energy of the melt is independent of temperature. Although valid for homopolymers this condition is not met by random copolymers. During fusion, the sequence distribution of crystallizable units will change with temperature. In turn, this will affect the free energy and chemical potential of the melt.[34,35] Hence, although the principles involved in deriving eq 1 are correct, the restrictions imposed by copolymer melting do not allow the use of the Gibbs–Thomson equation in the simplified form given.

The insensitivity of the calculated distribution to heating rates can be attributed to at least two factors. One possibility is lack of any significant superheating that could be attributed to the low levels of crystallinity of random copolymers. The other involves the insensitivity of eq 1 to small crystallite thicknesses which are characteristic of random copolymers. This insensitivity is reflected in the analysis of Figure 4. Focusing attention on the solid line, appropriate to sample F and Figures 8 and 10, we find that when the melting range is far removed from the equilibrium melting temperature, the crystallite thickness is small and relatively insensitive to large changes in the observed melting temperature. Thus, the calculated thickness for sample F, which melts in a wide temperature range from 70 to 105 °C (far from the equilibrium melting temperature of 137.5 °C), is very narrow, varying only from 40 to 90 Å approximately. For the copolymer studied in Figure 9 the observed melting temperature is 98 °C which is 37 deg below the equilibrium melting temperature. Hence, in the vicinity of a $T_m \simeq 100$ °C large changes in temperature result in only small changes in thickness which explains the insensitivity of the calculated distribution to changes in the heating rate of ethylene copolymers, as shown in the example of Figure 9. In contrast, for linear polyethylene the temperatures involved in the endotherm are much closer to the equilibrium melting temperature. The differences between the observed and equilibrium melting temperature are only about 12 deg in this case. Thus, according to the dashed curve in Figure 4, in the vicinity of 135 °C large changes in crystallite thicknesses should result with small changes in temperature.

In summary, we have found that despite its growing popularity the indirect determination of the crystallite thickness distribution by applying the Gibbs–Thomson equation to the melting curve obtained from differential scanning calorimetry is not generally applicable. This conclusion is reached by comparing for the first time the calculated distributions with those directly obtained by independent methods. For linear polyethylene, the direct experimentally measured distribution can only be reproduced by choosing appropriate combinations of the interfacial free energy and the heating rate. Even when the interfacial free energy is determined independently,[9,13] the choice of heating rate still remains arbitrary.

The distributions calculated from endotherms of random ethylene copolymers are very different from those that are obtained directly. Possible reasons for the large discrepancy have been discussed above. However, central

to the problem is the nature of the fusion process typical of random copolymers.

Acknowledgment. This work was supported by the Polymer Program Grant DMR 89-14167 of the National Science Foundation.

References and Notes

(1) Voigt-Martin, I. G.; Stack, G. M.; Peacock, A. J.; Mandelkern, L. *J. Polym. Sci., Polym. Phys. Ed.* **1989**, *27*, 957.
(2) Voigt-Martin, I. G.; Mandelkern, L. *J. Polym. Sci., Polym. Phys. Ed.* **1989**, *27*, 967.
(3) Voigt-Martin, I. G.; Alamo, R.; Mandelkern, L. *J. Polym. Sci., Polym. Phys. Ed.* **1986**, *24*, 1283.
(4) Snyder, R. G.; Scherer, J. R. *J. Polym. Sci., Polym. Phys. Ed.* **1980**, *18*, 1421.
(5) Glotin, M.; Mandelkern, L. *J. Polym. Sci., Polym. Lett. Ed.* **1983**, *21*, 807.
(6) Stack, G. M.; Mandelkern, L.; Voigt-Martin, I. G. *Polym. Bull.* **1982**, *8*, 421.
(7) Zachmann, H. G.; Stribeck, N.; Alamo, R. G.; Mandelkern, L. Manuscript in preparation.
(8) Gibbs, J. H. In *Collected Works*; Longman Green & Co.: Essex, U.K., 1928.
(9) Wlochowicz, A.; Eder, M. *Polymer* **1984**, *25*, 1268.
(10) Alberola, N.; Cavaille, J. Y.; Perez, J. *J. Polym. Sci., Polym. Phys. Ed.* **1990**, *28*, 569.
(11) Mills, P. J.; Hay, J. N. *Polymer* **1984**, *25*, 1277.
(12) Bodor, G.; Dalcolmo, H. J.; Schröter, O. *Colloid. Polym. Sci.* **1989**, *267*, 480.
(13) Darras, O.; Séguéla, R. *Polymer* **1993**, *34*, 2946.
(14) Hoffman, J. D.; Lauritzen, J., Jr. *J. Res. Natl. Bur. Stand.* **1961**, *65A*, 276.
(15) Hoffman, J. D. *Soc. Plast. Eng. Trans.* **1964**, *4*, 315.
(16) Hosoda, S. *Polym. J.* **1988**, *20*, 383.
(17) Jadav, S.; Jain, P. C.; Namda, V. S. *Thermochim. Acta* **1985**, *84*, 141.
(18) Kawai, T.; Hosoi, M.; Kamide, K. *Makromol. Chem.* **1971**, *146*, 55.
(19) Ottani, S.; Porter, R. S. *J. Polym. Sci., Polym. Phys. Ed.* **1991**, *29*, 1179.
(20) Alamo, R. G.; Mandelkern, L. *Macromolecules* **1989**, *22*, 1273.
(21) Alamo, R. G.; Viers, B. D.; Mandelkern, L. *Macromolecules* **1993**, *26*, 5740.
(22) Flory, P. J.; Vrij, A. *J. Am. Chem. Soc.* **1963**, *85*, 3548.
(23) Quinn, F. A., Jr.; Mandelkern, L. *J. Am. Chem. Soc.* **1958**, *80*, 3178.
(24) Strobl, R. G.; Eckel, R. *J. Polym. Sci., Polym. Phys. Ed.* **1976**, *14*, 913.
(25) Voigt-Martin, I. G.; Mandelkern, L. *J. Polym. Sci., Polym. Phys. Ed.* **1984**, *22*, 1901.
(26) Voigt-Martin, I. G.; Fischer, E. W.; Mandelkern, L. *J. Polym. Sci., Polym. Phys. Ed.* **1980**, *18*, 2347.
(27) Voigt-Martin, I. G.; Mandelkern, L. *J. Polym. Sci., Polym. Phys. Ed.* **1981**, *19*, 1769.
(28) Mandelkern, L.; Prasad, A.; Alamo, R. G.; Stack, G. M. *Macromolecules* **1990**, *23*, 3696.
(29) Mandelkern, L.; Stack, G. M.; Mathieu, P. J. M. *Anal. Calorim.* **1984**, *5*, 223.
(30) Alamo, R.; Mandelkern, L. *J. Polym. Sci., Polym. Phys. Ed.* **1986**, *24*, 2087.
(31) Alamo, R.; Domszy, R.; Mandelkern, L. *J. Phys. Chem.* **1984**, *88*, 6587.
(32) Alamo, R. G.; Mandelkern, L. *Thermochim. Acta* **1994**, *238*, 155.
(33) Flory, P. J. *J. Chem. Phys.* **1949**, *17*, 223.
(34) Flory, P. J. *Trans. Faraday Soc.* **1955**, *51*, 848.
(35) Alamo, R. G.; Chan, E. K. M.; Mandelkern, L.; Voigt-Martin, I. G. *Macromolecules* **1992**, *25*, 6381.
(36) Voigt-Martin, I. G.; Mandelkern, L. In *Handbook of Polymer Science and Technology*; Cheremisinoff, N. P., Ed.; Marcel Dekker Publishers: 1989; Vol. 3, p 1.
(37) Contrary to many reports in the literature[32] they also concluded that the ethyl branches enter the crystal lattice. This conclusion was based on the apparently high $T_m°$ values obtained from an extrapolation of the T_m versus $1/L_C$ data reported by Martuscelli et al.[38] on similarly constituted copolymers compared to those predicted according to Flory's theory. However, to calculate the predicted value, the $T_m°$ for the linear polyethylene chain was taken as 140 °C. If a higher value is taken, for example $T_m°$ = 145.5 °C,[22,29,39] the predicted $T_m°$ for the copolymers will be very close to the value obtained experimentally. In addition to the long extrapolation involved, the compositions of the copolymers were not obtained by any direct analytical method.[13] Furthermore, the extrapolated melting temperatures were compared with those calculated from theory, which involves the assumption of random sequence distribution.[33,34] The sequence distribution of the ethylene–butene copolymers studied in these two works[13,38] must be far from random. The reason is that the reported melting temperatures and core thicknesses of these copolymers are much higher than those obtained in model hydrogenated poly(butadienes).[20,31,35] The hydrogenated poly(butadienes) and ethylene–butene copolymers, which have a homogeneous composition and random distribution of ethyl branches, follow the same melting temperature–composition relation. Because this relation is identical to that followed by other random copolymers with bulkier branches (such as butyl, hexyl, and acetate), it can be concluded that ehtyl or longer branches are excluded from the lattice.[20,31,32,40] The melting temperatures of compositional heterogeneous ethylene copolymers, as well as those deviating from random sequence distribution, are known to be much higher than those having random distribution.[20,31] This appears to be the reason for the high extrapolated equilibrium melting temperatures that were obtained.
(38) Martuscelli, E.; Pracella, M. *Polymer* **1974**, *15*, 306.
(39) Weeks, J. J. *J. Res. Natl. Bur. Stand.* **1963**, *A67*, 441.
(40) Richardson, M. J.; Flory, P. J.; Jackson, J. B. *Polymer* **1963**, *4*, 221.